Rich structural polymorphism of monolayer polymeric C_{60} from cluster rotation

Xueao Li,* Fan Zhang,* Xuefei Wang, Weiwei Gao,† and Jijun Zhao
Key Laboratory of Material Modification by Laser, Ion and Electron Beams (Dalian University of Technology), Ministry of Education, Dalian 116024, China

(Received 28 April 2023; accepted 9 October 2023; published 3 November 2023)

The recent experimental fabrication of monolayer and few-layer C_{60} polymers paves the way for synthesizing two-dimensional (2D) cluster-assembled materials. Compared to individual atoms, clusters as superatoms (e.g., C_{60}) have an additional rotational degree of freedom, greatly enriching the phase spaces of superatom-assembled materials. Using first-principles calculations, we investigate a series of quasitetragonal and quasihexagonal polymeric C_{60} monolayers which are related by cluster rotation. The energy barriers of cluster rotation in quasitetragonal monolayer C_{60} structures are rather low (about 10 meV/atom). The small rotational energy barrier leads to a series of tetragonal C_{60} polymorphs with energies that are close to the experimental quasitetragonal phase. Similarly, several dynamically stable quasihexagonal monolayer C_{60} structures are found to have energies within 7 meV/atom higher than the experimental quasihexagonal phase. Our calculations demonstrate photoexcited electron-hole pairs and electrostatic doping of electrons can effectively modulate the relative energies of quasitetragonal C_{60} polymorphs, while the relative energies of different quasihexagonal polymorphs are insensitive to electrostatic doping of electrons. The experimental quasitetragonal phase, which is not dynamically stable in its monolayer form, can be stabilized when it is electrostatically doped with electrons.

DOI: 10.1103/PhysRevMaterials.7.114001

I. INTRODUCTION

Conventionally, atoms are considered as fundamental building blocks of materials. However, analyzing or designing materials by examining the chemical interactions between atoms as well as the numerous possible combinations of elements is not always the most convenient route. Many materials can be considered as assemblies of "superatoms" [1–4], which are structurally stable entities (or clusters) consisting of strongly bounded atoms and show chemical behavior similar to an individual atom [5–9]. The concept of a superatom not only provides a new perspective on cluster-assembled materials, but also opens up new avenues for exploring the building blocks of novel functional materials [3,10].

Among cluster-based superatoms, C_{60} buckminsterfullerene has been widely studied due to several desirable properties [11–13]. First of all, C_{60} is one of the few nanoclusters that can be mass produced in high quality [14]. It exhibits exceptional stability under high temperature and a wide range of chemical environments, making it a promising building block of cluster-assembled materials [15]. Bulk C_{60}-based crystal has a rich temperature-pressure phase diagram [16]. Under ambient conditions, the C_{60} solid is a face-centered cubic (fcc) solid bounded by van der Waals (vdW) interaction [17]. Under suitable pressure and temperature, C_{60} solids undergo a series of phase transitions to different carbon allotropes, such as quasi-low-dimensional polymers with tetragonal or hexagonal cells [18,19], disordered states [20], simple cubic phase [20–22], and many more [23,24]. Theoretically, several two-dimensional (2D) C_{60} polymers have also been proposed [25–28], while synthesis of these monolayer C_{60} crystals has proven challenging. Recently, researchers successfully synthesized 2D polymeric C_{60} single crystals, namely, quasihexagonal (qH) phase and quasitetragonal (qT) phase C_{60}, by removing Mg^{2+} ions from magnesium fulleride Mg_4C_{60} or Mg_2C_{60}, respectively [29,30]. However, only the monolayer qH phase was achieved, while the qT phase was synthesized as a few-layer material [29,30].

Unlike an individual atom, which is invariant under rotations about its center, clusters or superatoms have an additional rotational degree of freedom. This additional degree of freedom extends the available phase space and affects the physical properties of cluster-based materials. C_{60} clusters, for example, rotate freely in the fcc phase at ambient temperature but are fixed in an ordered orientation in the simple cubic phase between 100 and 260 K [22]. Below 85 K, the orientations of C_{60} molecules are frozen disorderedly in a glassy state [20,22,31]. Quasi-one-dimensional (1D) and 2D C_{60} phases have also been proposed to show various C_{60} orientations and physical properties [32–34]. Moreover, the interaction between various substrates and adsorbed fullerenes are significant and can stabilize C_{60} in ordered directions [35–38]. Overall, earlier experiments mainly focus on samples where C_{60}'s are bounded via vdW interactions. It is not clear whether and how C_{60} rotates in the recently discovered monolayer C_{60} [29,30], where fullerenes are bounded via covalent bonds.

In this work, we investigated the energies and structural properties of monolayer quasihexagonal and quasitetragonal polymeric C_{60} polymorphs that are related by rotating C_{60}.

*These authors contributed equally to this work.
†weiweigao@dlut.edu.cn

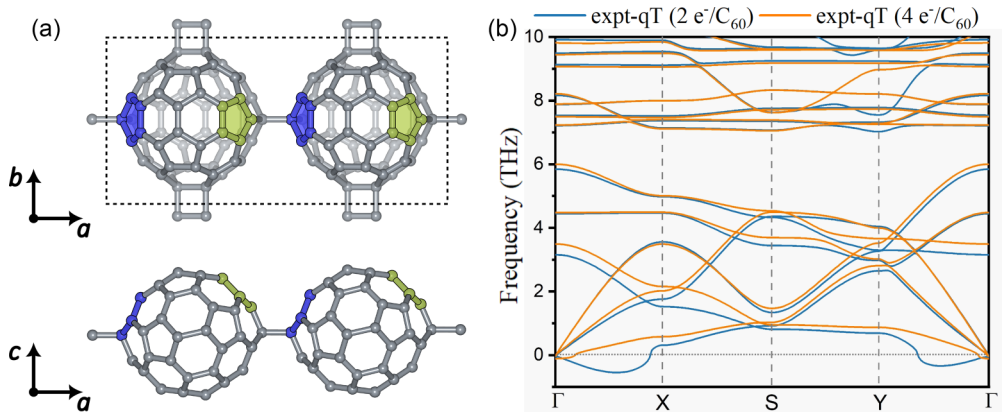

FIG. 1. (a) The top and side views of the experimentally synthesized few-layer quasitetragonal (expt-qT) phase. Pentagons are highlighted with colors to show the orientation of C_{60} clusters. (b) Phonon spectra of monolayer expt-qT phase doped with 2 and 4 electrons per C_{60}. For clarity, only phonon modes with frequencies lower than 10 THz are shown.

Similar to bulk phases of C_{60}-based crystals bonded with vdW interaction, C_{60} fullerenes in the monolayer polymeric quasitetragonal phases have low rotating energy barriers, suggesting the coexistence of different polymorphs or even orientationally disordered states. Electrostatic doping of electrons and optically excited electron-hole pairs effectively switch the relative energies and induce phase transitions between quasitetragonal polymorphs. Different from quasitetragonal phases, monolayer quasihexagonal phases are insensitive to electrostatic doping and have more rigid frameworks, which hinders the rotation of C_{60} fullerenes.

II. COMPUTATION METHODS

Density functional theory (DFT) calculations were performed using the plane-wave basis and the projector augmented wave approach as implemented by the Vienna *ab initio* simulation package (VASP 5.4.4) [39]. We used the Perdew-Burke-Ernzerhof (PBE) functional [40] and the D3 correction [41] to treat exchange-correlation effects and dispersion interaction, respectively. The configuration of valence electrons considered in PAW potentials for C is $2s^2\,2p^2$. A plane-wave cutoff of 400 eV, and a $3 \times 3 \times 1$ Monkhorst-Pack $k-$point mesh for both qT and qH structures were used [42]. To model charged monolayer C_{60}, we set the out-of-plane lattice parameter c to 75 Å, which corresponds to the vacuum layer thickness of ~ 68 Å. Tests of convergence with respect to lattice parameter c are presented in Fig. S7 and discussions in the Supplemental Material [43]. All structures were optimized until the energy differences between consecutive ionic steps were less than 10^{-4} eV/supercell and the force felt by each atom was less than 0.01 eV/Å. Phonon dispersions were calculated in the PHONOPY [44] package via the frozen-phonon method. The VESTA [45] package was used for the illustration of atomic structures. We performed nudged elastic band (NEB) [46,47] calculations using VTST [48] (Transition State Tools for VASP). In the NEB part, the electronic structure was calculated with an energy cutoff of 400 eV. The convergence threshold for the electronic energy was set to 10^{-5} eV, while the threshold for the ionic forces was set to 0.03 eV/Å, and the energy profile was obtained by interpolating the energies of the intermediate states.

III. RESULTS AND DISCUSSIONS

As shown in Fig. 1(a), the experimental quasitetragonal phase (abbreviated as "expt-qT" hereafter) has mixed types of intercluster bonds, including $[2+2]$ cycloaddition bonds connecting C_{60} clusters along the b direction and single C-C bonds connecting C_{60} along the a direction [29]. Fully structural optimization of the monolayer expt-qT phase shows that the C-C single bonds along the a direction are broken, resulting in periodically arranged 1D chainlike (abbreviated as "1D-chain") C_{60} polymers with $[2+2]$ cycloaddition bonds along the b direction. Similarly, the experiments did not report a viable synthesis of monolayer expt-qT C_{60} [29] and recent computational work also suggests that the monolayer expt-qT structure is unstable [49].

The experimentally synthesized few-layer quasitetragonal C_{60} polymers are prepared from Mg_2 C_{60}, which crystallizes in a monoclinic space group $I2/m$. Given that C_{60} is an electron acceptor in fullerides [50], one might expect that the expt-qT structure might be stabilized under conditions of electrostatic electron doping. To put this hypothesis to the test, we found that electrostatically doping the expt-qT phase with 1.25 electrons per C_{60} keeps the C-C single bonds intact during structural relaxation. The stability of the expt-qT polymer can be further confirmed by checking the phonon dispersion under doping conditions. As shown in Fig. 1(b), the monolayer expt-qT structure has imaginary phonon modes in a small region around the Γ point when it is doped with 2 electrons/C_{60}. As the doping electron concentration further increases to 4 electrons/C_{60}, the imaginary phonon modes are absent.

To gain deeper understanding of the energy landscapes of quasitetragonal monolayer C_{60} polymers, we compared expt-qT with 1D-chain as mentioned above and another tetragonal polymeric C_{60} monolayer (named the qT-E phase for brevity) [19,51,52], which has [2+2] cycloaddition bonds bridging C_{60} clusters along both the a and b directions. The energies of qT-E, expt-qT, and 1D-chain structures with respect to the lattice

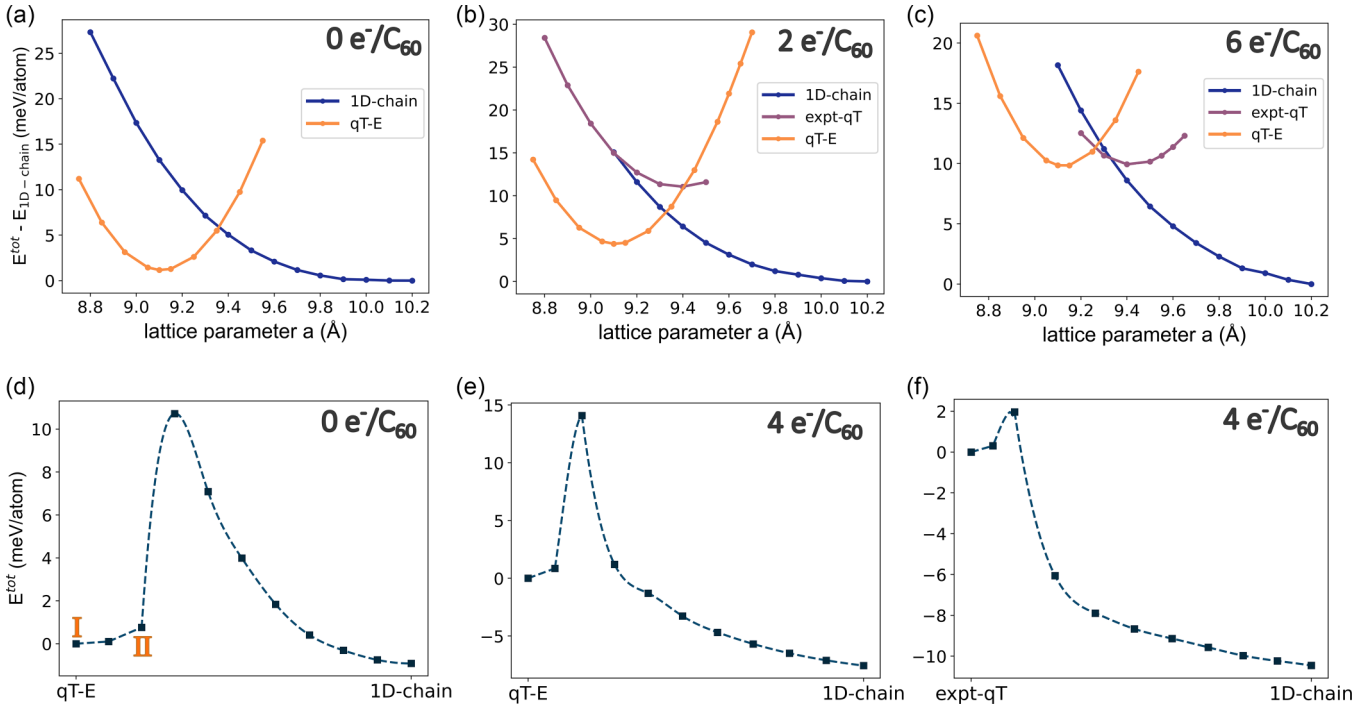

FIG. 2. (a)–(c) The energies of expt-qT, qT-E, and 1D chain versus the lattice parameter a with electrostatically doping electrons of 0, 2, and 6 electrons per C_{60}, respectively. (d), (e) The changes in energy along the transition path from qT-E to 1D-chain structure when the material is doped with 0 and 4 electrons per C_{60}, respectively. (f) The changes in energy along the transition path from expt-qT to 1D chain with an electron doping concentration of 4 per C_{60}. The corresponding structural change diagram is shown in Fig. S3 of the Supplemental Material [43].

constant a for a series of electron doping concentrations are presented in Figs. 2(a)–2(c), where the energy of the 1D-chain structure is set as the reference. For electron concentrations ranging from 0 to $6\,e^-/C_{60}$, the energy of the 1D chain is lower than those of the expt-qT and qT-E phases. Under the undoped condition, the energy curve of the expt-qT superimposes with that of the 1D chain and does not show a local minimum for lattice constant a less than 9.6 Å. This suggests the expt-qT phase directly decomposes to 1D chain without electron doping. As the electron concentration increases to $2\,e^-/C_{60}$, a local minimum (or saddle point) appears in the energy curve of the expt-qT phase. The local minimum has higher energy than the qT-E phase by about 7 meV/atom. As the electron concentration increases to more than 6 e^-/C_{60}, the energy of the expt-qT phase becomes lower than that of the qT-E phase. The reversal of relative energy ordering between the qT-E and expt-qT structures suggests that doping electrons can potentially induce a structural transition between these two polymorphs.

We calculated the energy barriers between qT-E, qT-expt, and 1D-chain polymorphs using the NEB method [46,47]. The structural changes between these three structures mainly involve the rotation of C_{60} clusters around the b axis. Figures 2(d) and 2(e) show the energy changes along the transition path from qTP-E to 1D-chain structure under undoped and doped conditions, respectively, with schematic plots of initial, intermediate, and final structures. During the transition, the intercluster bonds along the a direction of qTP-E are broken in the first few steps, leading to a drastic energy increase, which is then followed by a gradual transition to 1D-chain structure. The energy barrier between qT-E and 1D chain in the undoped case is approximately 11 meV/atom, which increases to 14 meV per atom upon doping $4\,e^-/C_{60}$. Similarly, Fig. 2(f) shows the energy changes along the transition from expt-qT to the 1D-chain structure under the $4\,e^-/C_{60}$ doping condition. The energy barrier between expt-qT and 1D chain is only 2 meV/atom. Such a small transition barrier is lower than the rotation energy barrier of fullerene (about 6 meV/atom) in the face-centered cubic C_{60} solid with vdW intercluster interaction (the calculated rotation barriers and rotation process are as shown in Figs. S1 and S2 in the Supplemental Material [43]). In other words, the monolayer expt-qT structure can only exist at low temperature even if it is doped with electrons. At the ambient condition, thermal fluctuation can trigger a structural transition from expt-qT to 1D-chain or qT-E structure.

The small rotating energy barrier of C_{60} in the quasitetragonal structures suggests the possibility of alternative polymorphs composed of fullerene clusters in different combinations of orientations. We examined polymorphs that contain combinations of three possible orientations of C_{60} clusters, labeled as I–III, which appear in expt-qT and qT-E structures. Note that I and III are related by a mirror-reflection symmetry operation with respect to the bc plane, as shown in Fig. 3(a). A collection of C_{60} polymeric quasitetragonal (qT) allotropes, labeled as qT-A, B, C, D, E, F, and G structures, are illustrated in Fig. 3(b). We optimized the structures of these quasitetragonal C_{60} polymers and compared their energies under undoped and electrostatic doping conditions. Here the highest simulated carrier doping concentration is around

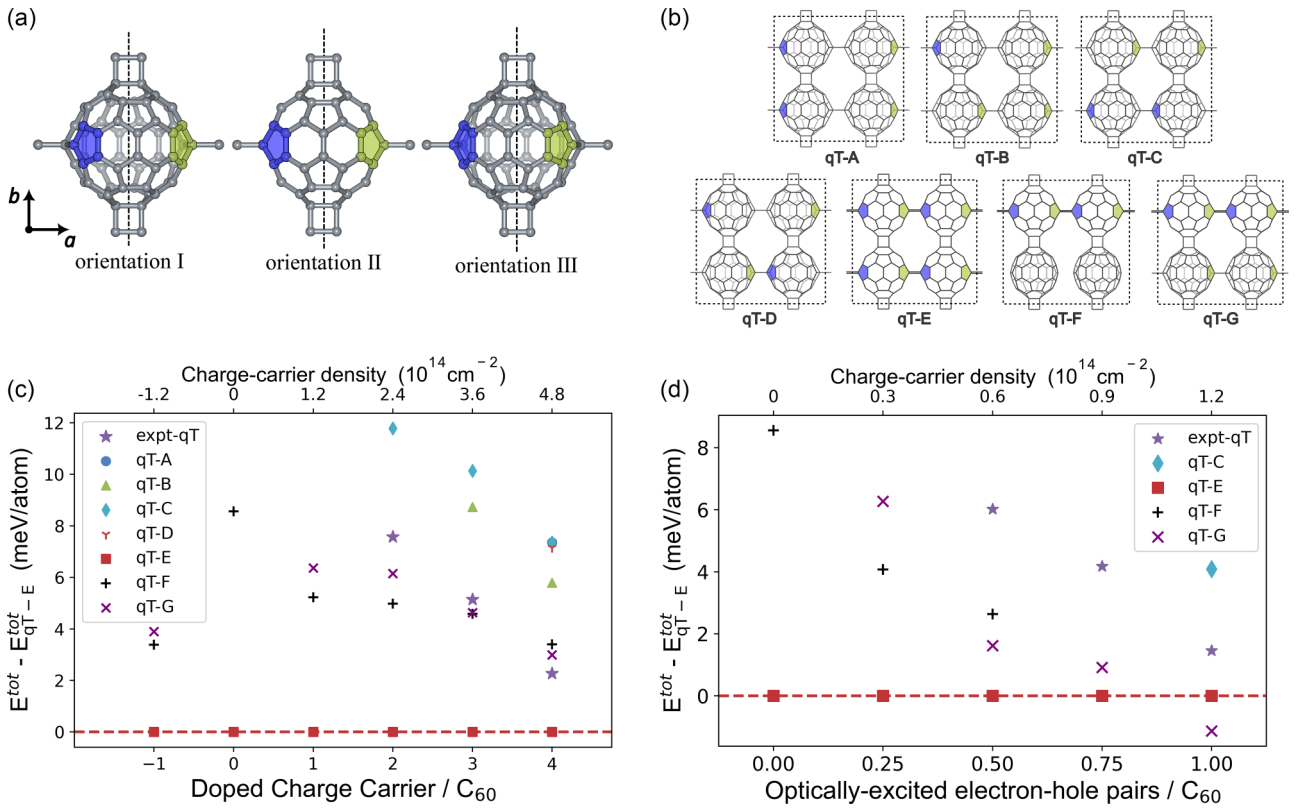

FIG. 3. (a) Possible orientations of C_{60} in quasitetragonal (qT) structures. Orientations I and III are related by mirror reflection about the *bc* plane. (b) The top views of monolayer qT-A, qT-B, qT-C, qT-D, qT-E, qT-F, and qT-G polymorphs which consist of combinations of various C_{60} orientations. (c) Relative energies per atom of qT structures at doping conditions. (d) Relative energies of quasitetragonal polymorphs when 0, 0.25, 0.5, 0.75, and 1 electron-hole pairs per C_{60} are excited. Here, we only plot the data points that are converged in DFT structural optimization. The energy of the qT-E structure is used as a reference.

$4.8\times\ 10^{14}\,\mathrm{cm}^{-2}$, which is achievable in 2D materials with gate-induced electrostatic doping [53]. As shown in Fig. 3(c), among these monolayer qT polymorphs, the qT-E structure remains the ground state for doping-carrier concentration in the range of $1-4\,e^-/C_{60}$. The qT-A, B, C, and D structures can exist in a limited range of electron doping concentrations and have slightly higher energy compared to the expt-qT phase. Interestingly, with doping-carrier concentration in range of $1-3\,e^-/C_{60}$, both qT-F and qT-G structures have lower energies than the expt-qT phase. Speaking overall, the energy differences between these tetragonal structures are small (less than 12 meV/atom), indicating the coexistence of several qT phases or even an orientational glass state in a 2D quasitetragonal C_{60} polymer.

The impact of electrostatic doping on qT polymorphs and strong light-matter coupling in ultrathin materials motivates us to investigate the effects of optically excited electron-hole pairs on qT polymorphs. Previous experiments reported light-induced phenomena of C_{60}-based materials, such as photoinduced polymerization of C_{60} [54,55] and photoinduced superconductivity in fullerides [56]. Here we use the delta self-consistent field method to simulate effects of depopulating the highest occupied bands and populating the lowest unoccupied bands [57,58]. By comparing the energies of qT structures, we found the relative energies of qT polymorphs also sensitively depend on the concentration of photoexcited electrons and holes, as shown in Fig. 3(d). For instance, the expt-qT structure becomes stable and its energy relative to the qT-E structure decreases as the number of excited electrons per C_{60} increases. When there is less than one electron-hole pair doped for each C_{60}, the qT-E becomes the ground state. When one electron-hole pair per C_{60} (i.e., 1.2×10^{14} cm^{-2}) is excited, qT-G becomes approximately 2 meV/atom lower than the qT-E structure. In other words, the qT-G structure that is unstable in the undoped condition may be stabilized when optically excited electron-hole concentration reaches around $1\times\ 10^{14}\,\mathrm{cm}^{-2}$, which is on the same order of magnitude as that experimentally achieved in monolayer transition metal dichalcogenides [59,60].

Different from few-layer expt-qT, the experimental quasihexagonal (qH) phase (abbreviated as expt-qH) is synthesized from Mg_4 C_{60}, where each C_{60} unit is covalently bonded with six neighboring clusters. The C_{60} clusters have two orientations in the expt-qH phase, which can be distinguished by examining the pentagon on the top of C_{60}, as highlighted in Fig. 4(a). The C_{60} clusters bonded via [2+2] cycloaddition bonds along the $\vec{a}$ axis have the same orientation, while C_{60} clusters bonded via C-C single bonds along the $\vec{b}+\vec{a}$ or $\vec{b}-\vec{a}$ directions are oriented in another direction. Similar to the tetragonal phases, various quasihexagonal structures that combine different C_{60} orientations can exist. In addition to the expt-qT structure, we considered three

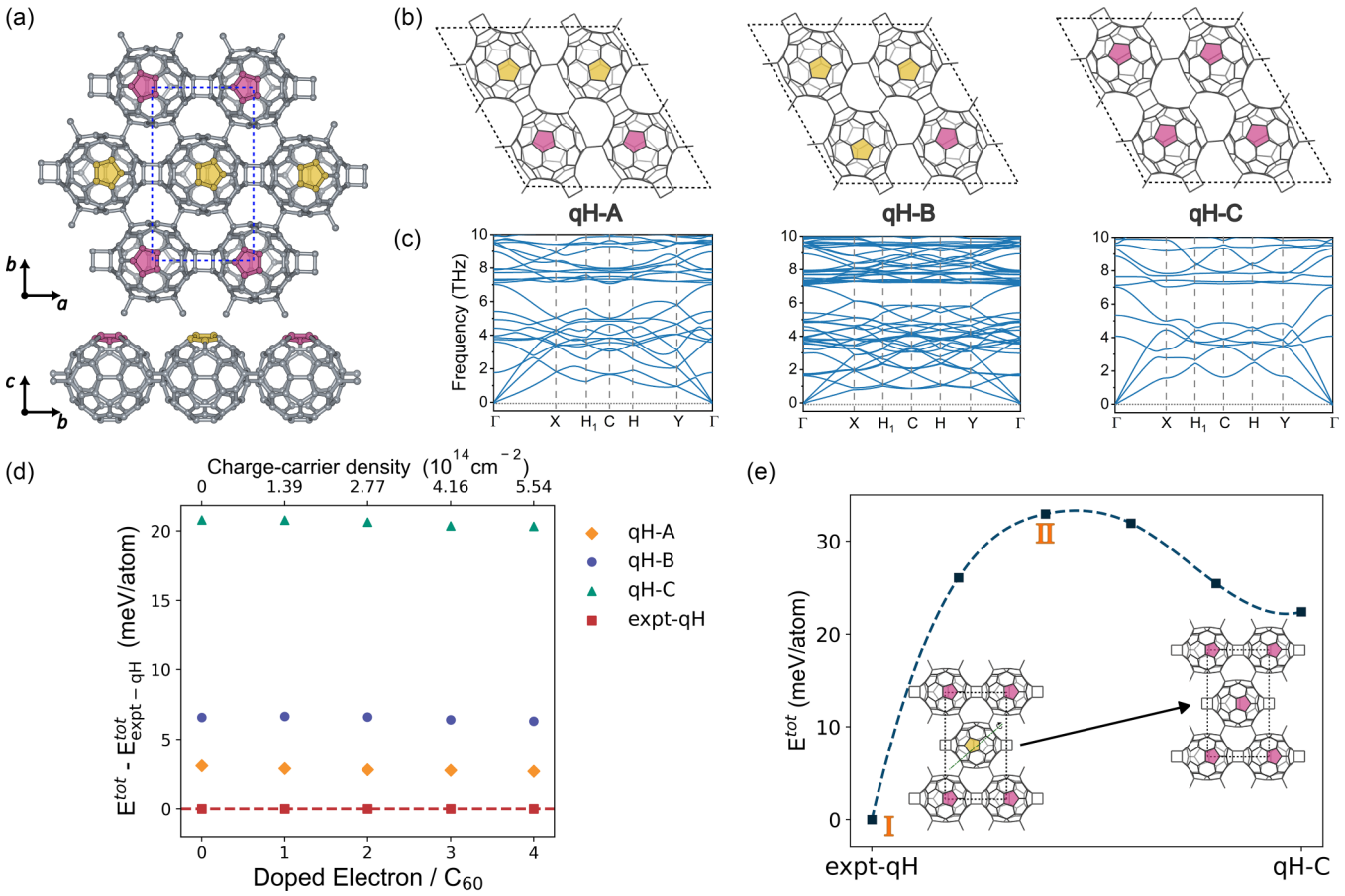

FIG. 4. (a) The top and side views of experimental quasihexagonal (qH) structures. The top pentagons are highlighted in colors to illustrate two different C_{60} orientations. (b) Several quasihexagonal polymorphs constructed by combining two orientations of C_{60} clusters. These qH polymorphs are denoted as qH-A, qH-B, and qH-C. (c) Phonon dispersions of qH polymorphs under undoped conditions. For clarity, only phonon modes with frequencies lower than 10 THz are shown. (d) Relative energies per atom of qH-A, qH-B, qH-C, and expt-qH. The expt-qH structure is set to be the reference. When doped with one e^- per C_{60}, the corresponding doped carrier density is about 1.39×10^{14} cm^{-2}. (e) The changes in energy along the transition from expt-qH to qH-C structure.

potential quasihexagonal monolayer C_{60}, denoted as qH-A, qH-B, and qH-C, phases. Figure 4(b) schematically displays these four qH structures and highlights the top pentagons to better distinguish them. Figure 4(c) shows the phonon dispersions of monolayer qH-A, B, and C structures, which are all free of imaginary modes signifying their dynamic stability. The band structures of four qH polymorphs are presented in Supplemental Material Fig. S6 [43], showing band gaps in the range from 0.44 to 0.70 eV from PBE calculations. In other words, the rotational degree of freedom of C_{60} in these materials is an effective knob for tuning the electronic and optical properties.

With electrostatic doping of electrons [Fig. 4(d)], the relative energies of four qH structures remain nearly the same, which is in stark contrast to the large doping-induced changes of the relative energies between quasitetragonal polymorphs. The expt-qH structure remains the ground state when the doping-carrier concentration is between 0 and $4\,e^-/C_{60}$. qH-A and qH-C polymorphs are close in energy and about 3 meV/atom above that of the expt-qH structure, while the energies of the qH-B and qH-C structures are 7 and 21 meV/atom higher than the expt-qH structure, respectively. Using the NEB method, we calculate the energy barrier for rotating a C_{60} cluster in the expt-qH structure. As shown in Fig. 4(e), the energy barrier for C_{60} rotation in the expt-qH structure is more than 30 meV/atom, much higher than that in quasitetragonal structures. The higher-energy barrier can be qualitatively explained by the fact that rotating C_{60} in the expt-qH structure breaks more intercluster bonds than the cases of qT structures.

To better understand the distinctive doping effects on qH and qT polymorphs, we analyzed the changes of charge density distribution between the undoped condition and the $4\,e^-/C_{60}$ doping condition. As highlighted by the dashed lines in Fig. 5(a), the charge density for doped electron substantially accumulates at the C-C single bond along the a direction of the expt-qT structure when it is doped with electrons. Such charge accumulation strengthens the C-C single bonds and thereby enhances the stability of the expt-qT structure. By examining the charge density changes of other qT structures, we find electron doping has mixed effects on the C-C bonds along the a direction in different qT polymorphs (as shown in Supplemental Fig. S4 [43]), resulting in evident doping-induced changes of their relative energies. Different from qT

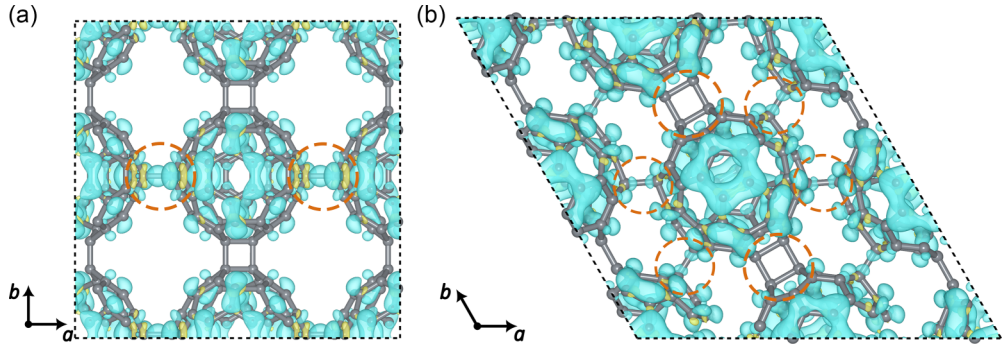

FIG. 5. (a) The charge density difference between the undoped state and that doped with 4 electrons per C_{60} for expt-qT. (b) The charge density difference between undoped state and the state doped with 4 electrons per C_{60} for expt-qH. The cyan and yellow isosurfaces correspond to charge density changes of 0.001 05 e Bohr^{-3} and $-0.001\,05\,e$ Bohr^{-3}, respectively.

polymorphs, electron doping introduces a small accumulation of charge density at the inter-C_{60} bonds of all qH structures (as shown in Supplemental Fig. S5 [43]). As highlighted by the dashed lines in Fig. 5(b), doped electrons contribute little near the intercluster bonds in the expt-qH structure. In other words, electrostatic doping has minor effects on the intercluster covalent bonds in qH C_{60} polymers, and hence leads to a limited impact on the relative energies of qH polymorphs.

To find phonons that contribute the most to structural changes between qH or qT polymorphs of monolayer C_{60}, we decompose changes of atomic coordinates $\Delta\boldsymbol{R} = \boldsymbol{R}_{\mathbf{I}} - \boldsymbol{R}_{\mathbf{II}}$ with zone-center phonon modes $\boldsymbol{u}_\alpha$, where α is the index of phonon modes [61,62]. $\boldsymbol{R}_{\mathbf{I}}$ and $\boldsymbol{R}_{\mathbf{II}}$ are the atomic coordinates of structures I and II chosen from the NEB transition path, as shown in Figs. 2(d) and 4(e). The projection of structural changes $\Delta\boldsymbol{R}$ to phonon mode α is given by $\eta_\alpha = \frac{\Delta\boldsymbol{R}}{|\Delta\boldsymbol{R}|} \cdot \boldsymbol{u}_\alpha$. Figures 6(a) and 6(b) show spheres with radii proportional to $|\eta_\alpha|^2$ on top of the phonon spectra of the qT-E and expt-qH phases, respectively. For the transition from qT-E to 1D chain, low-energy optical phonon modes around 8 THz contribute the most, while for the transition from expt-qH to qH-C, the phonon modes between 5 and 45 THz contribute almost evenly. These results indicate that the transition between qT-E and 1D chain may be triggered by perturbing the qT-E structure with a smaller number of phonon modes around 8 THz, while it is more difficult for the transition between expt-qH and qH-C to happen when phonon modes in a narrow frequency range are excited.

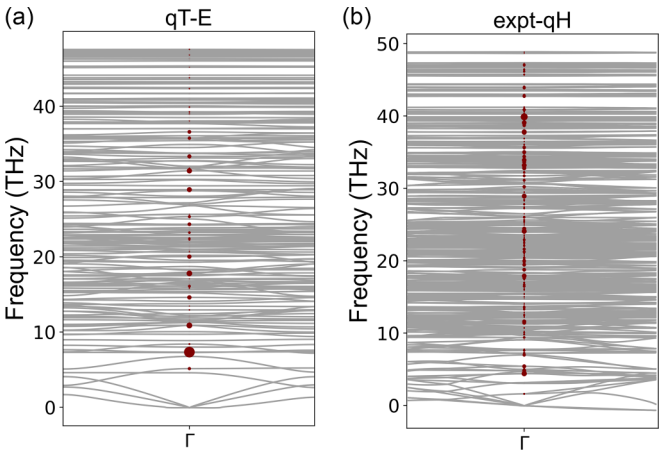

FIG. 6. (a) Phonon spectra of qT-E and contribution of phonon eigenvalues at Γ points. (b) Phonon spectra of expt-qH and contribution of phonon eigenvalues at Γ points. The radii of the colored spheres in the figure are proportional to $|\eta_\alpha|^2$.

IV. CONCLUSIONS

Our study broadens the family of fullerene-assembled 2D materials that are related by rotating constituent C_{60} superatoms. We show that electrostatic and optically excited electron-hole pairs effectively tune the relative energies of qT polymorphs. In particular, the monolayer expt-qT structure, which is dynamically unstable at the undoped condition, can be stabilized by electrostatically doping with electrons. The energy barriers of rotating C_{60} clusters in monolayer quasitetragonal polymorphs are lower than those of quasihexagonal phases, suggesting a mixture of several qT structures or a glass state with C_{60} oriented disorderedly. Several quasihexagonal polymorphs with dynamic stability and energies close to those of expt-qH are also proposed. Different from qT structures, the relative energies between qH structures cannot be effectively changed by electron doping. In addition to doping, we envision metal surfaces, which interact strongly with adsorbed C_{60} molecules, as a promising platform for stabilizing various polymeric C_{60}'s. The impacts of metal substrates on the structure, electronic, and optical properties of polymeric C_{60} thin films are of potential technological interest and deserve further experimental and theoretical investigations.

ACKNOWLEDGMENTS

This work is supported by the National Natural Science Foundation of China (Grants No. 12104080 and No. 91961204) and the Fundamental Research Funds for the Central Universities (Grants No. DUT22LK04 and No. DUT22ZD103). The authors acknowledge the computer resources provided by the Supercomputing Center of Dalian University of Technology, Shanghai Supercomputer Center, and Sugon supercomputer centers.

[1] S. N. Khanna and P. Jena, Phys. Rev. Lett. **69**, 1664 (1992).
[2] S. N. Khanna and P. Jena, Phys. Rev. B **51**, 13705 (1995).
[3] P. Jena and Q. Sun, Chem. Rev. **118**, 5755 (2018).
[4] E. A. Doud, A. Voevodin, T. J. Hochuli, A. M. Champsaur, C. Nuckolls, and X. Roy, Nat. Rev. Mater. **5**, 371 (2020).
[5] D. E. Bergeron, A. W. Castleman, Jr., T. Morisato, and S. N. Khanna, Science **304**, 84 (2004).
[6] G. L. Gutsev and A. I. Boldyrev, Chem. Phys. **56**, 277 (1981).
[7] G. L. Gutsev and A. I. Boldyrev, Chem. Phys. Lett. **92**, 262 (1982).
[8] P. Jena, J. Phys. Chem. Lett. **6**, 1119 (2015).
[9] P. Jena, J. Phys. Chem. Lett. **4**, 1432 (2013).
[10] J. U. Reveles, P. A. Clayborne, A. C. Reber, S. N. Khanna, K. Pradhan, P. Sen, and M. R. Pederson, Nat. Chem. **1**, 310 (2009).
[11] D. Cox, S. Behal, M. Disko, S. Gorun, M. Greaney, C. Hsu, E. Kollin, J. Millar, and J. Robbins, J. Am. Chem. Soc. **113**, 2940 (1991).
[12] W. Krätschmer, L. D. Lamb, K. Fostiropoulos, and D. R. Huffman, Nature (London) **347**, 354 (1990).
[13] H. W. Kroto, J. R. Heath, S. C. O'Brien, R. F. Curl, and R. E. Smalley, Nature (London) **318**, 162 (1985).
[14] R. Haufler, J. Conceicao, L. Chibante, Y. Chai, N. Byrne, S. Flanagan, M. Haley, S. C. O'Brien, and C. Pan, J. Phys. Chem. **94**, 8634 (1990).
[15] S. Tomita, J. U. Andersen, K. Hansen, and P. Hvelplund, Chem. Phys. Lett. **382**, 120 (2003).
[16] M. Álvarez-Murga and J. Hodeau, Carbon **82**, 381 (2015).
[17] P. A. Heiney, J. Phys. Chem. Solids **53**, 1333 (1992).
[18] Y. Iwasa, T. Arima, R. Fleming, T. Siegrist, O. Zhou, R. Haddon, L. Rothberg, K. Lyons, H. Carter, Jr., and A. Hebard, Science **264**, 1570 (1994).
[19] M. Nunez-Regueiro, L. Marques, J.-L. Hodeau, O. Béthoux, and M. Perroux, Phys. Rev. Lett. **74**, 278 (1995).
[20] W. I. F. David, R. M. Ibberson, T. J. S. Dennis, J. P. Hare, and K. Prassides, Europhys. Lett. **18**, 219 (1992).
[21] F. Gugenberger, R. Heid, C. Meingast, P. Adelmann, M. Braun, H. Wühl, M. Haluska, and H. Kuzmany, Phys. Rev. Lett. **69**, 3774 (1992).
[22] P. A. Heiney, J. E. Fischer, A. R. McGhie, W. J. Romanow, A. M. Denenstein, J. P. McCauley Jr., A. B. Smith, and D. E. Cox, Phys. Rev. Lett. **66**, 2911 (1991).
[23] M. Yurovskaya and I. Trushkov, Russ. Chem. Bull. **51**, 367 (2002).
[24] B. W. Smith, M. Monthioux, and D. E. Luzzi, Chem. Phys. Lett. **315**, 31 (1999).
[25] J. Nakamura, T. Nakayama, S. Watanabe, and M. Aono, Phys. Rev. Lett. **87**, 048301 (2001).
[26] A. V. Okotrub, V. V. Belavin, L. G. Bulusheva, V. A. Davydov, T. L. Makarova, and D. Tománek, J. Chem. Phys. **115**, 5637 (2001).
[27] C. D. Reddy, Z. G. Yu, and Y.-W. Zhang, Sci. Rep. **5**, 12221 (2015).
[28] C. H. Xu and G. E. Scuseria, Phys. Rev. Lett. **74**, 274 (1995).
[29] L. Hou, X. Cui, B. Guan, S. Wang, R. Li, Y. Liu, D. Zhu, and J. Zheng, Nature (London) **606**, 507 (2022).
[30] E. Meirzadeh, A. M. Evans, M. Rezaee, M. Milich, C. J. Dionne, T. P. Darlington, S. T. Bao, A. K. Bartholomew, T. Handa, and D. J. Rizzo, Nature (London) **613**, 71 (2023).
[31] R. Blinc, J. Seliger, J. Dolinšek, and D. Arčon, Phys. Rev. B **49**, 4993 (1994).
[32] R. Moret, Acta Crystallogr. Sect. A Found. Adv. **61**, 62 (2005).
[33] J. Hou, Y. Jinlong, W. Haiqian, L. Qunxiang, Z. Changgan, Y. Lanfeng, W. Bing, D. Chen, and Z. Qingshi, Nature (London) **409**, 304 (2001).
[34] L.-F. Yuan, J. Yang, H. Wang, C. Zeng, Q. Li, B. Wang, J. G. Hou, Q. Zhu, and D. M. Chen, J. Am. Chem. Soc. **125**, 169 (2003).
[35] X. Lu, M. Grobis, K. H. Khoo, S. G. Louie, and M. F. Crommie, Phys. Rev. B **70**, 115418 (2004).
[36] J. Lu, P. S. E. Yeo, Y. Zheng, Z. Yang, Q. Bao, C. K. Gan, and K. P. Loh, ACS Nano **6**, 944 (2012).
[37] W. Chen, H. Zhang, H. Huang, L. Chen, and A. T. S. Wee, ACS Nano **2**, 693 (2008).
[38] E. J. G. Santos, D. Scullion, X. S. Chu, D. O. Li, N. P. Guisinger, and Q. H. Wang, Nanoscale **9**, 13245 (2017).
[39] G. Kresse and J. Furthmüller, Phys. Rev. B **54**, 11169 (1996).
[40] J. P. Perdew, K. Burke, and M. Ernzerhof, Phys. Rev. Lett. **77**, 3865 (1996).
[41] S. Grimme, J. Comput. Chem. **27**, 1787 (2006).
[42] H. J. Monkhorst and J. D. Pack, Phys. Rev. B **13**, 5188 (1976).
[43] See Supplemental Material at http://link.aps.org/supplemental/10.1103/PhysRevMaterials.7.114001 for the changes in energy along the transition path of rotating a C_{60} in fcc-C_{60}; the corresponding structure of fcc-C_{60} during the rotation; the detailed top view illustrating the distinct structural changes along the transition path corresponding to Figs. 2(d)–2(f); the top view of the charge density difference between the undoped state and 4 doped electrons per C_{60} for qT-E, qT-F, and qT-G; the top view of the charge density difference between the neutral state and 4 doped electrons per C_{60} for qH-A, qH-B, qH-C, and qH-D; the band structure of monolayer C_{60} polymorphs; and the energies of structures doped with four electrons per C_{60} calculated with different vacuum space.
[44] A. Togo and I. Tanaka, Scr. Mater. **108**, 1 (2015).
[45] K. Momma and F. Izumi, J. Appl. Crystallogr. **44**, 1272 (2011).
[46] G. Henkelman, B. P. Uberuaga, and H. Jónsson, J. Chem. Phys. **113**, 9901 (2000).
[47] D. Sheppard, P. Xiao, W. Chemelewski, D. D. Johnson, and G. Henkelman, J. Chem. Phys. **136**, 074103 (2012).
[48] Transition State Tools for VASP, http://theory.cm.utexas.edu/vtsttools/ (2010).
[49] B. Peng, Nano Lett. **23**, 652 (2023).
[50] B. Peng, J. Am. Chem. Soc. **144**, 19921 (2022).
[51] X. Chen and S. Yamanaka, Chem. Phys. Lett. **360**, 501 (2002).
[52] V. A. Davydov, L. S. Kashevarova, A. V. Rakhmanina, V. Agafonov, H. Allouchi, R. Ceolin, A. V. Dzyabchenko, V. M. Senyavin, and H. Szwarc, Phys. Rev. B **58**, 14786 (1998).
[53] Y. Wu, D. Li, C.-L. Wu, H. Y. Hwang, and Y. Cui, Nat. Rev. Mater. **8**, 41 (2023).
[54] A. Rao, P. Zhou, K.-A. Wang, G. Hager, J. Holden, Y. Wang, W.-T. Lee, X.-X. Bi, P. Eklund, and D. Cornett, Science **259**, 955 (1993).
[55] A. Ito, T. Morikawa, and T. Takahashi, Chem. Phys. Lett. **211**, 333 (1993).
[56] M. Budden, T. Gebert, M. Buzzi, G. Jotzu, E. Wang, T. Matsuyama, G. Meier, Y. Laplace, D. Pontiroli, M. Riccò *et al.*, Nat. Phys. **17**, 611 (2021).

[57] A. Hellman, B. Razaznejad, and B. I. Lundqvist, J. Chem. Phys. **120**, 4593 (2004).
[58] J. Gavnholt, T. Olsen, M. Engelund, and J. Schiøtz, Phys. Rev. B **78**, 075441 (2008).
[59] A. Chernikov, C. Ruppert, H. M. Hill, A. F. Rigosi, and T. F. Heinz, Nat. Photon. **9**, 466 (2015).
[60] B. Peng, H. Zhang, W. Chen, B. Hou, Z.-J. Qiu, H. Shao, H. Zhu, B. Monserrat, D. Fu, H. Weng *et al.*, npj 2D Mater. Appl. **4**, 14 (2020).
[61] A. Cammarata and T. Polcar, Phys. Rev. B **96**, 085406 (2017).
[62] W. Gao and J. R. Chelikowsky, Nano Lett. **20**, 8346 (2020).